Stability improvement of layered Au,Pt-YSZ mixed-potential gas sensing electrodes by cathodic polarization: Studies by steady state and dynamic electrochemical methods

X. Zhang [a,*], H. Kohler [a,*], M. Schwotzer [b], U. Guth [c]

[a] *Institute for Sensor and Information Systems, Karlsruhe University of Applied Sciences, Moltkestr. 30, D-76133, Karlsruhe, Germany*
[b] *Institute of Functional Interfaces, Karlsruhe Institute of Technology (KIT), Hermann-von-Helmholtz-Platz 1, D-76344, Eggenstein-Leopoldshafen, Karlsruhe, Germany*
[c] *Dresden University of Technology, Faculty of Chemistry and Food Chemistry, Bergstrasse 66c, D-01062, Dresden, Germany*

ABSTRACT

Electrochemical characteristics of a layered Au,Pt-YSZ mixed-potential (APE) gas sensing electrode were studied by open circuit potential (OCP) and electrochemical impedance measurements (EIS), especially in relation to effects of aging under ambient air conditions and cathodic polarization. Mixed-potential response of the APE to CO was found to be drastically reduced after 100 days of operation in ambient air, which is correlated with a clear change in the shape of the EIS characteristics and a considerably increased polarization resistance (R_p). By applying a cathodic polarization, the reduced sensitivity can be almost fully restored. Also the EIS characteristics tend to show a similar behavior as observed in the initial state. The influence of cathodic polarization treatment on the regeneration of the electrochemical (OCP and EIS) behaviors is found to be clearly enhanced at elevated temperatures (700 °C), while oxygen concentration seems to play no role on this regeneration effect. This polarization treatment will highly improve stability of the APE and is expected to enable applications like flue gas analysis.

1. Introduction

Solid state gas sensors using yttria-stabilized zirconia (YSZ) as solid electrolyte material have been intensively investigated during the last six decades, in particular with growing concerns to environmental issues, for instance exhaust pollutants from industries, combustion motor vehicles and even domestic fireplaces fueled with wood [1–19]. In most of these applications, the sensors are operated according to a thermodynamic working principle. Their sensing behaviors follow the Nernstian equation in a broad range of temperatures (400–1600 °C) and oxygen partial pressures (10 to 10^{-20} bar). Therefore they are denoted as Nernstian sensors [20–23].

Besides the Nernstian sensors, a special group of YSZ based sensors has attracted much attention, using a working principle, which is determined by reaction kinetics and known as the mixed potential mechanism. In the last two decades, this sensing concept gained high attraction due to its promising properties for in-situ analysis of combustible gas species at high-temperatures and a shortage of alternative sensor devices for those application purposes [2,5,16,17,24].

Especially, the continuous estimation of unburned or partly combusted components in flue gas of firewood combustion processes is still an unsolved problem, but is an essential task to enable advanced combustion air stream control concepts for an effective reduction of toxic emissions [16,17]. Unlike the mixed-potentials formed at electrodes in aqueous electrochemical systems, those generated on electrodes of YSZ based solid state electrochemical systems were observed to be even more stable [25]. In latest investigations of this type of sensors, the AuPt-mixtures admixed with YSZ fine powder were noted to be a promising mixed-potential electrode material. By using this electrode material combination, different mixed potential sensors were reported with satisfying sensing behaviors using various electrode designs [26–40]. Especially the sensing responses of a Au,Pt|YSZ layered mixed-potential gas sensing electrode (APE) were found to be strongly related to the catalytic properties of the electrode material, which were found to be clearly influenced by the Au/Pt ratio and the Au-distribution on Pt over the electrode layer [26,39–41].

However, as shown in our previous work, long term stability of this kind of APE was found to be not satisfying to fulfill e.g. the demands of

---

* Corresponding authors.
  E-mail addresses: xin.zhang@hs-karlsruhe.de (X. Zhang), heinz.kohler@hs-karlsruhe.de (H. Kohler).

operation in the flue gas from wood combustion processes [16,17]. In literature, instable sensing response of Au/AuPt-mixture based mixed-potential electrodes was attributed to i) re-crystallization of Au/AuPt-mixtures at the typical operation temperature of about 600 °C and ii) alteration of their catalytic properties due to irreversible gas reactions and poisoning effects [28,42].

On the other side, O_2,Pt|YSZ is one of the best-characterized solid-state electrochemical half-cells which has been extensively studied in various aspects [43–61]. These investigations have revealed a wealth of knowledge of this type of solid state gas electrode. One of the important issues is the electrochemical mechanism of the oxygen transfer reaction at the O_2,Pt|YSZ electrode system owing to its fundamental relevance not only for scientific understanding but also for its performance in practical applications, for instance in oxygen sensors, solid oxide electrolysis cells (SOECs), solid oxide fuel cells (SOFCs), and non-faradic electrochemical modifications of catalytic activity in catalysis [62–68]. Different processes have been taken into account for clarification of the oxygen exchange mechanism. They include: i) adsorption of dissociative oxygen on electrode surface, ii) surface diffusion of atomic oxygen, and iii) charge transfer reactions proceeding at the triple-phase-boundary (tpb) [69,70].

Although plenty of remarkable research efforts have been exerted in the past, alterations at the O_2,Pt|YSZ electrode system by electrochemical treatments or aging processes at raised temperatures are still not entirely understood. These alterations are assumed to significantly affect the catalytic and electrochemical characteristics of the electrode, which therefore are needed to be further studied and clarified [43,46,55, 59,71–73]. The following changes have been proposed and discussed in the literature: i) accumulation/agglomeration of impurities and, accordingly, their segregation of the tpb, which are deemed as irreversible processes; ii) formation/decomposition of a platinum oxide (PtO_x) 'phase' at the O_2,Pt|YSZ electrodes, which is supposed to be a reversible process. Especially, the latter aspect was systematically investigated by various electrochemical methods in combination with different kinds of in-situ/ex-situ surface analytical approaches [43,46, 55,59,71]. As a result, PtO_x formation was postulated to occur at different regions within the electrode system, including: i) the interface between Pt and YSZ, ii) the tpb O_2,Pt|YSZ, and iii) the Pt metallic surface, i.e. the interface between Pt and O_2 [43,46,55,71].

Moreover, it was found that anodic polarization was able to promote the formation of PtO_x, and its extent was strongly related to temperature, oxygen partial pressure and oxygen flux towards the electrode during polarization. On the other hand, a decomposition of the pre-formed PtO_x was demonstrated to be favored via an electro-chemical reduction under the condition of cathodic polarization [46,71]. These changes of the O_2,Pt|YSZ electrode, i.e. the formation/decomposition of PtO_x by anodic/cathodic polarization, can clearly change the catalytic properties and kinetics of the electrode, and influence the corresponding electrode processes as well.

Likewise, the Pt|YSZ based mixed-potential electrode modified by Au addition may probably undergo similar changes as stated above. As a result, long-term sensing stability of this type of electrode can be highly influenced by those changes in the micro- and nano-structure of the electrode, in particular the ones occurring during aging processes at elevated temperatures. It has to be also noted that, the electrochemical treatments, e.g. the anodic and the cathodic polarization, are expected to induce the structural changes of the electrode as well. This would consequently change the catalytic properties and electrochemical characteristics of the electrode, and accordingly take influence on its gas sensing behaviors. However, there is almost no literature available in the field of mixed potential type gas sensors, which reveals the correlations between the structural changes of the electrodes induced by thermal treatment during aging process or electrochemical treatments and their sensing characteristics, especially in relation to the long term sensing stability.

The considerations stated above motivated this work to study aging effects on layered Au,Pt|YSZ mixed-potential gas sensing electrodes by open circuit potentiometry (OCP), cyclic voltammetry (CV) and electrochemical impedance spectroscopy (EIS). In a second step, the same comparative studies were applied again to study the role of cathodic polarization on the electrochemical behaviors of the APEs, in particular with relation to their gas sensitivity and sensing stability over a long term of operation. The changes of the OCP and EIS characteristics before and after the aging process, as well as after regeneration of the aged electrodes by cathodic polarization, are discussed in context with reversible / irreversible changes at the tpb of the electrodes.

2. Experimental

2.1. Sensor element

Commercially available sensor elements (CarboSen, LAMTEC GmbH, Walldorf, Germany) in planar design are investigated in this work. Such a sensor element is comprised of two identical layered APE on top of a porous YSZ layer, a buried Pt reference electrode (Pt-RE) located between an alumina substrate and the porous YSZ-layer, and a Pt heater placed on the reverse side of the substrate, as schematically shown in Fig. 1a. The design of two identical APEs on a single sensor element is aimed to build up a redundant measuring system for increasing reliability. However, all the measurements/analysis in this work were only carried out on the right-hand APE of different sensor individuals. As shown in Fig. 1b, the APE itself consists of a screen printed thick-film Pt-electrode covered by a thin-film Au layer using PVD technique, and was subsequently sintered at 1050 °C for 240 min. More technical details of this kind of sensor elements are described in [26,40].

2.2. Investigation of long-term mixed potential stability

Long term mixed potential stability was investigated by open circuit potential (OCP), electrochemical impedance spectroscopy (EIS) and cyclic voltammetry (CV) measurements, which were complemented by studies of electrode morphology using an environmental scanning electron microscopy (ESEM). The OCP and the CV measurements were carried out using an automated gas mixing system [28] outfitted with an electrochemical work station PalmSens3 (PalmSens, The Netherlands). The surface morphological structures of APEs were studied with an ESEM type XL 30 FEG, (Philips Inc., The Netherland) equipped with an EDX system.

Sensing behaviors (OCP response) of the sensors were studied by measuring the potential difference (ΔU) between the APE and the Pt-RE, as illustrated in Fig. 1a. The sensors were characterized at 600 °C under exposure to 1000 ppm CO balanced with synthetic air.

EIS characteristics of the sensors were investigated using a two-electrode arrangement (Fig. 1a). In the EIS analysis, voltages in sinusoidal form with an amplitude of 10 mV at varying frequencies from 10 kHz to 10 mHz were applied on the Au,Pt-YSZ|YSZ|Pt cell to study its EIS characteristics under ambient air conditions. This EIS characteristic is deemed to be composed of an interfacial impedance (electrode|electrolyte) and a bulk impedance from solid electrolyte [74].

With respect to the stability tests, a fresh sensor element (1#) was continuously operated at 600 °C for 100 days under ambient air conditions (aging process). The CO responses of sensor 1# were studied by OCP measurements under exposure to a CO/synthetic air mixture (c (CO) 1000 ppm) at 600 °C on the 1st, 47th and 100th day. The corresponding EIS characteristics on those three measurement days were recorded under the same temperature condition but only with exposure to synthetic air. Moreover in order to study the aging effect on electrode morphology, the ESEM analyses on the APE were conducted before the aging process and after the sensor operation of 100 days. Besides the application of these measurement sequences, the sensor element (1#) was operated at 600 °C in ambient air all the time over these 100 days.
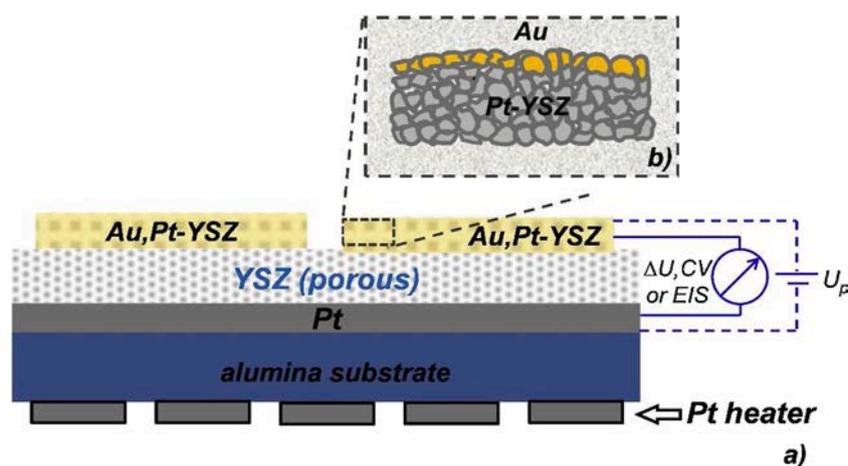
Fig. 1. Schematic cross-section of a) the CarboSen sensor element with the electrical wiring arrangement for OCP/EIS measurements (blue solid line) and electrode polarization treatments (blue dashed line), and b) of the structure of the layered Au,Pt-YSZ mixed potential sensing electrode (For interpretation of the references to colour in this figure legend, the reader is referred to the web version of this article.).

2.3. Cathodic treatment for sensing response regeneration

After the aging period (100 days) at 600 °C and ambient air conditions as described above, a sensitivity regeneration procedure was applied to the sensor 1# in two sequential steps: i) the operation temperature of the sensor was elevated to 700 °C in synthetic air for 2 h; ii) the APE was cathodically polarized using a two-electrode configuration (Fig. 1a blue dashed line) in a temperature range from 600 to 700 °C. During the processes of cathodic polarization (step ii), cyclic potential sweeps between φ_e (the equilibrium potential, about 0 mV) and -0.6 V at a scan rate of 50 mV/s were imposed to the Au,Pt,-YSZ|YSZ|Pt cell under 5 vol.% O_2 at 600, 650 and 700 °C, separately. Further details of this procedure are given in Fig. 7.

After the step of heating-up at 700 °C for 2 h (step i) and each cathodic polarization treatment at those three different temperatures (step ii), the electrochemical characteristics of the sensors were estimated by OCP and EIS measurements under the same experimental conditions as described in Sec. 2.2. Finally, the ESEM analysis on the APE of the sensor 1#, which underwent all the measurements/treatments as stated above, was performed again to check whether a morphological change of that APE occurred by aging and/or cathodic polarization.

Furthermore, in order to better distinguish the role of gaseous oxygen concentration with respect to the sensitivity regeneration, another sensor individual (2#) underwent also an aging process in ambient air at 600 °C for about 3 months. After that, this sensor element was regenerated by imposing the cyclic cathodic polarization to the layered Au,Pt-YSZ electrode again at 700 °C, but now in synthetic air (20.5 vol.% O_2). The OCP responses to 1000 ppm CO were separately characterized before the aging process, after aging for about three months and finally at the end subsequent to the cathodic treatment.

3. Results and discussion

3.1. Effect of aging on OCP sensing response

The sensing responses of sensor 1# to CO at 600 °C in different phases of the experiment are shown in Fig. 2. Before use in these stability tests, this sensor element was only stored at room temperature under ambient air condition. The OCP response (ΔU, see Sec. 2.2) was found to be about 66 mV at 1000 ppm CO balanced with synthetic air on the 1st day. This value was marginally raised to 62 mV after operating the sensor at 600 °C in ambient air for 47 days. Subsequent to another 53 days of operation under the same conditions (600 °C, ambient air), a
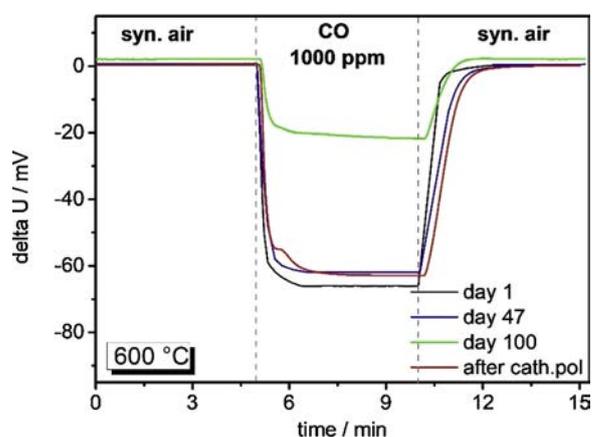
Fig. 2. OCP response to CO at 600 °C on the 1 st, 47th and 100th day, and after cathodic polarization (C.P.) on the APE of sensor 1#.

significant decrease of the response to approx. 22 mV was surprisingly measured after a total operation time of 100 days, which was only 33 % of the initial response. Besides, a slight shift of the baseline measured in synthetic air was noted to be positively varied from 0.3 mV to 2.1 mV (Fig. 2).

The ΔU measured in the experiments is the potential difference between the APE|YSZ half-cell and the Pt|YSZ reference half-cell (φ_{Pt} φ_{APE}, Fig. 1). The potential formed at the Pt|YSZ half-cell ought to follow a Nernstian characteristic at 600 °C. Since the YSZ layer of the sensor shows a porous morphology [26], it is presumed that the gas atmosphere in the vicinity of the buried reference half-cell Pt|YSZ is in thermo-dynamic equilibrium with the ambient atmosphere. In these experiments, the oxygen concentration was kept at 20 vol.%, and the CO concentration used was only 1000 ppm. Therefore, it can be assumed that the Nernstian potential at the Pt|YSZ half-cell is almost the same in synthetic air compared to that at 1000 ppm CO balanced with synthetic air. Consequently, the ΔU at 1000 ppm CO in synthetic air is deemed to be induced by the change of the potential at the APE|YSZ half-cell, which shows a non-Nernstian behavior under the CO exposure.

In the previous studies [26,28,40], the non-Nernstian behavior of this kind of layered Au,Pt-YSZ electrode was demonstrated to be a mixed-potential type. According to the theoretical model proposed in [42,75,76], the potential forming mechanism of the APE can be elucidated taking into account both, the gas phase oxidation of reducing gases within the electrode layer, and the electrochemical reactions at the

tpb (Fig. 3a). For further detailed discussion of this phenomenon, we consider a simplified case of the APE exposed to CO, O_2, N_2 model gas mixtures.

As schematically shown in Fig. 3a, the model gas mixture firstly passes through the porous APE-layer. In this process a gas phase reaction (CGR (1)) occurs, which consumes a portion of CO in a chemical way. The residual part of the CO, O_2, N_2 mixture arrives at the tpb, where the electrochemical oxidation of CO (EOC (2)) and the oxygen reduction reaction (ORR (3)) take place and make a direct electrochemical contribution to the mixed-potential formation. Under conditions of OCP-measurement (zero current conditions (Fig. 3b)) the mixed potential is established at the APE|YSZ half-cell. It represents a status of potential formation at which the electron transfer rate of the anodic reaction (EOC (2)) is equal to that of the cathodic reaction (ORR (3)). This means that the mixed-potential generated at the APE is a consequence of the balance of the rates of the gas phase reaction (CGR (1)), the anodic reaction (EOC (2)) and the cathodic reaction (ORR (3)) occurring at different locations of the electrode (Fig. 3a).

$$2CO + O_2 \rightarrow 2CO_2 \quad (CGR) \tag{1}$$

$$CO(g) + O_O^x(YSZ) \rightarrow CO_2(g) + V_O^{\circ\circ}(YSZ) + 2e \quad (APE) \quad (EOC) \tag{2}$$

$$\frac{1}{2}O_2(g) + V_O^{\circ\circ}(YSZ) + 2e \quad (APE) \rightarrow O_O^x(YSZ)(ORR) \tag{3}$$
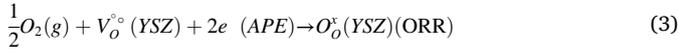
According to the Butler-Volmer equation, the current densities for the anodic (j_{CO}) and the cathodic (j_{O_2}) reaction can be expressed as follows (Miura's theory):

$$j_{CO} \quad j_{CO}^0 exp\{2\alpha_1 F(\varphi \quad \varphi_{CO}^0)/RT\} \tag{4}$$

$$j_{O_2} \quad j_{O_2}^0 exp\{ \quad 4\alpha_2 F(\varphi \quad \varphi_{O_2}^0)/RT\} \tag{5}$$

Here, φ represents the electrode potential, F is the Faraday constant, R is the molar gas constant, T is the temperature in Kelvin, φ^o denotes the equilibrium electrode potential of the correspondingly involved reaction (2) or (3), j_{CO}^0 and $j_{O_2}^0$ are the corresponding exchange current densities and α is the transfer coefficient [42,75]. Following the discussion above, the mixed potential formation at the tpb of the APE can be quantitatively derived as a function of CO and O_2 concentrations at the condition $|j_{CO}| \quad |j_{O_2}|$ or $j_{CO} + j_{O_2} \quad 0$, as given in Eq. (6) [77].

$$\varphi_m \quad \varphi_o + nA\ln c_{O_2} \quad mA\ln c_{CO} \tag{6}$$

where c signifies the concentration of CO and O_2, and φ_o, A, m and n are constants.

In other words, the mixed-potential can be schematically illustrated by intersections of the anodic and the cathodic curves by plotting the logarithm of the anodic current density (j_{CO}) and the negative logarithm of the cathodic current density (j_{O_2}) over the electrode potential φ, as

shown in Fig. 3b. Under synthetic air conditions the potentials generated on the mixed potential half-cell (APE/YSZ) and the reference half-cell (Pt/YSZ) are almost the same ($\varphi_{O_2}^{Pt} \approx \varphi_{O_2}^{APE}$), and correspondingly the ΔU ($\varphi_{O_2}^{APE} \quad \varphi_{O_2}^{Pt}$) is found to be approximately 0 mV as experimentally confirmed (Fig. 2). When CO is introduced into the gas atmosphere, the mixed potential (φ_m) formed at the APE would show a negative shift compared to the equilibrium potential ($\varphi_{O_2}^{APE}$) formed under synthetic air conditions (Fig. 3b). Consequently the ΔU ($\varphi_m \quad \varphi_{O_2}^{Pt}(\approx \varphi_{O_2}^{APE})$) is measured to be a negative value (Fig. 2). In addition, based on this discussion, we may infer that the mixed potential response is increased (a more negative shift of φ_m : ($\varphi_m^1 \rightarrow \varphi_m^2 \rightarrow \varphi_m^3 \rightarrow \varphi_m^4$)) by enhancing the anodic reaction and/or depressing the cathodic reaction, and decreased (the φ_m more positively shifted: ($\varphi_m^4 \rightarrow \varphi_m^3 \rightarrow \varphi_m^2 \rightarrow \varphi_m^1$)) by depressing the anodic reaction and/or enhancing the cathodic reaction, respectively (Fig. 3b).

3.2. Model of gas sensitivity depression by electrode aging effects

In order to gain a better description of the reasons for the depression of mixed-potential response after aging, the OCP measurements were complemented by EIS measurements conducted in synthetic air at 600 °C subsequent to each OCP test. The changes of the ΔU values (Fig. 2) were found to be in good correlation with the changes of the EIS characteristics, as shown in Fig. 4. A quasi-semicircle was measured on the 1st day in synthetic air at 600 °C. The corresponding polarization resistance (R_p) was estimated to be approximately 7 kΩ. After 47 days operation at 600 °C in ambient air, the EIS characteristic under the same conditions could still hold the shape of a quasi-semicircle, but the R_p was noted to be enlarged to about 35 kΩ. Surprisingly, the Nyquist plot showed only an incomplete semicircle after 100 days. The R_p was observed to be significantly raised to about 430 kΩ (Fig. 4a), which was estimated by a numerical complementation of that incomplete semi-circle. This shows a drastic increase compared to those R_p measured before. As a two-electrode configuration was used in the EIS measure-ments (Sec. 2.2), the polarization resistances are not only related to the APE|YSZ interface but also to the Pt-RE|YSZ interface. But due to the higher catalytic activity and the much larger size of the Pt-RE compared to the APE, it is assumed that the polarization resistances in the EIS measurements are dominated by the APE|YSZ electrode, and mainly represent the status of the APE|YSZ interface.

After a number of cycles of negative potential sweeps to the APE (Sec. 2.3), the ΔU response to the 1000 ppm CO/air mixture and the baseline in synthetic air (Fig. 2) were almost recovered to the values measured on the 47th day. In addition, after this polarization procedure the EIS characteristic was restored to a state very similar to that on the 47th day (Fig. 4b). This recovering effect on the OCP and the EIS characteristics of the APE by cyclic cathodic polarization was found to be highly affected by both the temperature and the number of potential

Fig. 3. a) Schematic representation of the electrode processes involved in the mixed potential formation, taking CO balanced with O_2/N_2 as an example. b) Illustration of the mixed potential formation in four different situations according to the differences in the kinetics of the anodic and the cathodic reaction, respectively.
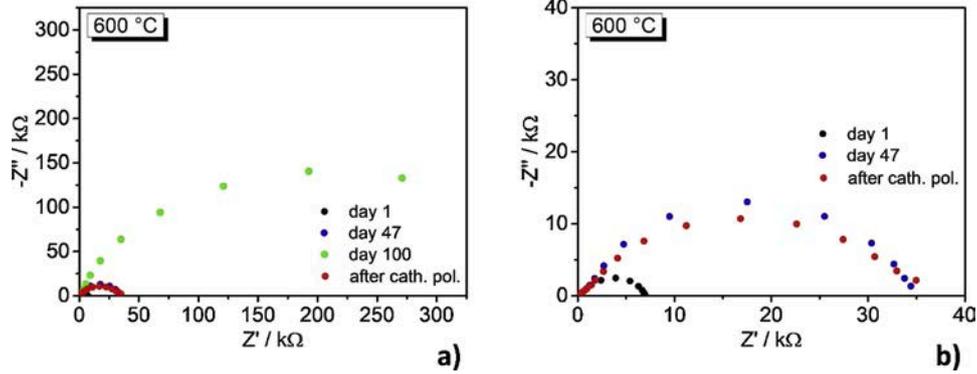
Fig. 4. Overview a) of EIS characteristics in ambient air at 600 °C on the 1st, 47th and 100th day, and after polarization of the APE (sensor 1#), and the corresponding zoomed view b) of the EIS-behaviors change from day 1 to day 47.

scans. Details of this aspect will be discussed in Sec. 3.3.

Moreover from the ESEM analyses on the APE, no clear electrode morphological changes, in terms of grain size and porosity, can be found by either the aging process at 600 °C under ambient air conditions (Cf. Fig. 5 a and b) or the application of the cathodic polarization (Cf. Fig. 5 b and c). This means, neither the changes of the electrochemical characteristics (OCP and EIS) of the APE by aging nor those ones by cathodic polarization treatment can be attributed to the morphological changes of the electrodes. This result is different from the results reported in literature [42,46,47,59]. In this context, it can be inferred that only the state of the triple phase boundary (tpb) of the APE, i.e. the location of potential formation, but not the electrode morphology is altered by operation of the sensor in ambient air at 600 °C over these 100 days. The changes of the tpb in the first 47 days resulted in a weaker effect on the electrochemical characteristics of the APE. This is indicated by a mild rise of R_p and only a little response decrease to CO as observed in the EIS- and the OCP-measurements, respectively (Fig. 2 & 4). But the further development of these changes from 47th day to 100th day considerably changed the electrochemical characteristics of the electrode. This is reflected by a drastic rising of R_p (Fig. 4) and, accordingly, a significant degradation of OCP response (Fig. 2). Only very similar electrochemical behaviors (OCP response (Fig. 2) and EIS characteristics (Fig. 4)) of the APE to those on 47th day could be recovered by the application of the negative potential scans. However, a complete regeneration to the initial characteristics as measured on 1st day was not achieved with this procedure.

From the experimental facts stated above we may conclude that the aging process relates to both, irreversible and reversible changes at the APE|YSZ interface, as schematically illustrated in Fig. 6 a, b & c. Hypothetically, agglomeration of impurities at the electrode|electrolyte interface (Fig. 6 b) might be the origin of the irreversible changes and the reversible changes are likely attributed to oxidation processes and formation of an additional oxide phase at the metallic parts of the tpb (Fig. 6c) [46,71–73].

According to the results reported in [46,71,72], these irreversible

and reversible changes at the APE|YSZ interface are assumed to lead to a descent of the concentration of the active electrochemical reaction sites at the tpb. This would consequently affect the anodic and the cathodic processes (EOC 2 and ORR 3) proceeding at the tpb, and accordingly depress the mixed-potential formation (Figs. 2 and 3b).

With respect to the influence of the blockage of the reaction sites on the electrochemical processes proceeding at the tpb, the increased R_p after sensor aging (Fig. 4) verifies a reduced electrode kinetics for the oxygen reduction reaction (ORR, (3)) by the aging process, because the R_p characterized in synthetic air is a direct measure of the exchange current density for the ORR ($j_{O_2}^0$). According to the model introduced above (Fig. 3b), the decrease of the ORR kinetics would result in a more negative potential shift at the Au,Pt-YSZ electrode due to the enhancement of mixed potential formation when 1000 ppm CO is introduced, under the assumption that the EOC kinetics is kept unchanged. However for the aged APE, the mixed-potential response is found to be not increased but rather reduced (Fig. 2), even though the ORR kinetics at this electrode is experimentally confirmed to be decreased. These facts indicate that at the aged APE, i) the kinetics of the electrochemical oxidation of CO (EOC, (2)) after the sensor aging is depressed as well, and the extent of the kinetics reduction of the EOC is larger than that of the ORR, as illustrated in Fig. 6d.

On the other hand, the not complete regeneration of the mixed-potential response ($\varphi_m^{100} \rightarrow \varphi_m^{reg.} \approx \varphi_m^{47}$) and the EIS characteristic ($R_p^{100} \rightarrow R_p^{reg.} \approx R_p^{47}$) after the application of negative potential scans (Figs. 2 and 4) is probably an indication that only the oxidized metallic parts of the tpb but not the agglomeration of impurities at the APE|YSZ interface can be recovered by cathodic polarization. The regeneration effects are assumed to be limited to the electrochemical reduction process of the oxidized metallic parts of the APE to the metallic state driven by cathodic polarization, as shown in Fig. 6 b→c. The corresponding blocked reaction sites at the tpb are postulated to be reactivated by this electrochemical reduction process, and accordingly an enhanced electrode kinetics for the EOC (reaction 2) and the ORR (reaction 3) can be
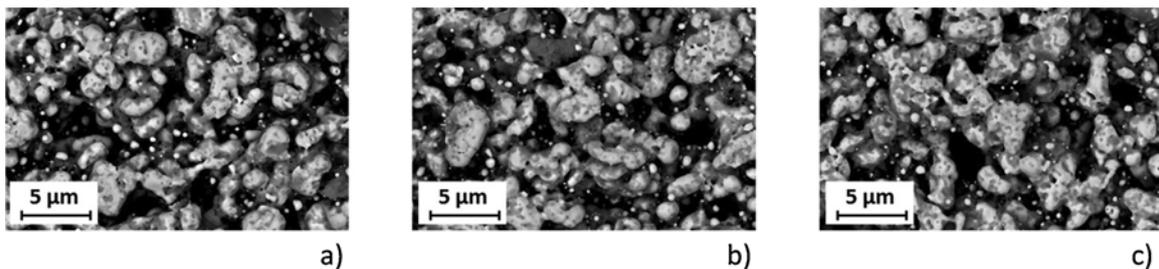
Fig. 5. ESEM images of the layered Au,Pt-YSZ electrode a) before operation, b) after aging at ambient air for 100 days and eventually c) after the cathodic polarization treatment.
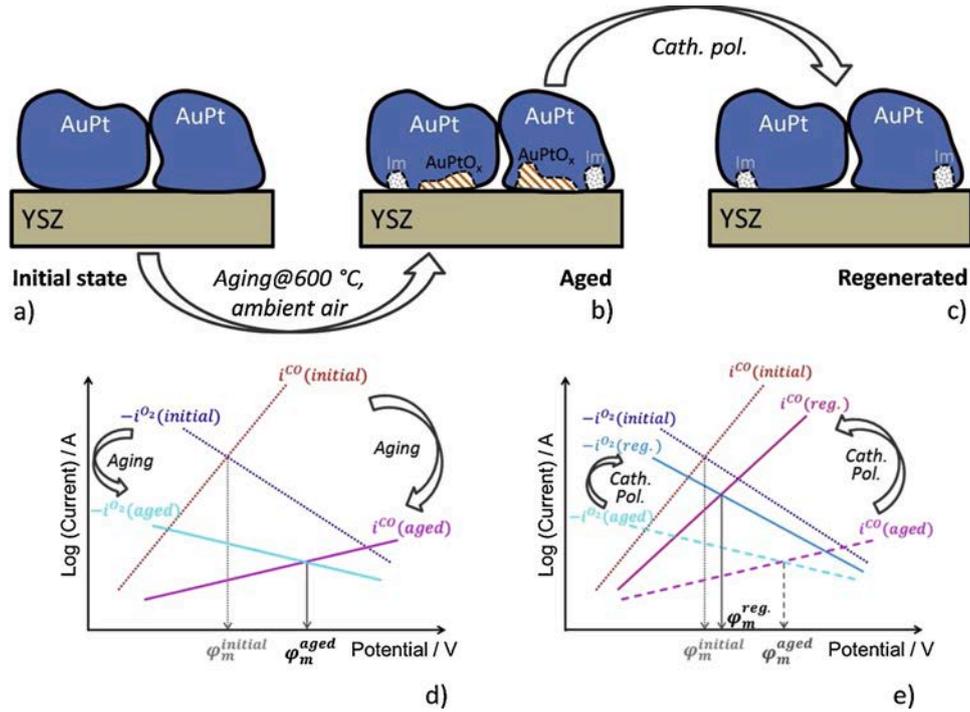
Fig. 6. Illustration of the hypothetical oxidation of the APE|YSZ interface and the accumulation of impurities by sensor aging (a → b), and the corresponding electrochemical reduction process by cathodic polarization (b → c). Schematic representations of mixed potential formation at the aged (d) and the regenerated state (e) of the APE with different electrode kinetics, respectively.
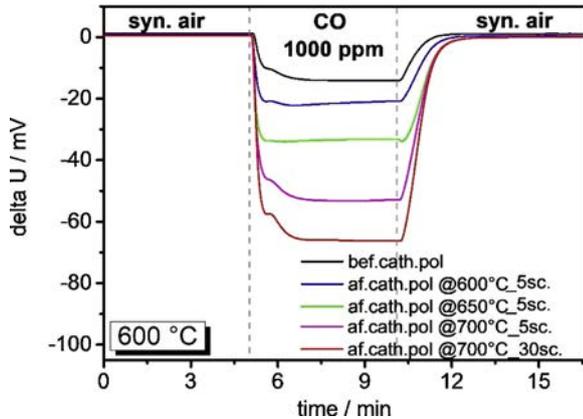
Fig. 7. OCP responses of the aged sensor (1#) at 1000 ppm CO balanced with synthetic air before and after cathodic polarization (af. cath. pol.) at 600, 650 and 700 °C, separately.

expected compared to that of the aged APE (Fig. 6e). In full accordance with this model, very similar OCP (Fig. 2) and EIS behaviors (Fig. 4) are measured after the electrochemical reduction compared to those observed on the 47th day.

3.3. Regeneration of OCP sensing response by cathodic polarization at different temperatures

After the degradation of response by a 100 days' aging procedure at 600 °C in ambient air (Sec. 2.2), a regeneration of sensing response to CO was found to be achieved by applying cyclic cathodic polarization on the APE (Sec. 2.3). It was revealed by further experiments that not only the temperature at which the polarization is carried out but also the number of potential sweeps take an essential influence on the efficiency of the response recovery procedure.

As shown in Fig. 7, the OCP responses of the aged sensor (1#) to 1000 ppm CO in air was noted to be enhanced with different extent after the cathodic polarization sequences at different temperatures between 600–700 °C at 5 vol.% O_2. A mild rising of the OCP response to CO can be already observed by cathodically polarizing the APE with five scans in the range between 0 and -0.6 V at 600 °C. The gas sensitivity is further enhanced by increasing the temperature during further polarization sequences in steps at 650 °C and finally 700 °C. The cathodic polarization treatments were also carried out with five potential scans at each of these two temperatures. Interestingly, the response is even again elevated to nearly the initial value measured before the aging process by another 25 potential sweeps at the final temperature (700 °C) (Fig. 7). With regard to the development of the sensitivities to 1000 ppm CO (Fig. 7), it has to be noted that this almost complete regeneration of the sensing response is reached only by a sufficient number of sweeps at 700 °C (five sweeps are not enough), rather by a possible accumulative effect of all the electrochemical treatments applied to this sensor individual.

In accordance with other electrochemical studies on Pt|YSZ and Au|YSZ interfaces in [46,55,59,71,72,78] it is postulated that the application of cathodic polarization on the APE does not only result in the oxygen reduction reaction (ORR 3, Sec. 3.1) but also induces the electrochemical reduction of the oxidized metallic parts of the tpb at the APE (Fig. 6b→c). This may be described by the following reaction:

$$AuPtO_x + 2xe^- \rightarrow AuPt + xO^{2-} \tag{7}$$

Those oxidized metallic parts of the tpb are supposed to be formed in the foregoing aging process, as illustrated in Fig. 6a→b.

This would again release those blocked electrochemical reaction sites due to formation of $AuPtO_x$, and accordingly increase the concentration of the active reaction sites at the tbp. The charge transfer processes (Fig. 6e) proceeding there would be consequently enhanced, namely both the anodic and the cathodic reactions contributing to the formation of the mixed potential. As a result, a stronger (more negative) mixed potential is formed at the electrode, as stated in Sec. 3.2.

With regard to the role of the temperature, the better response enhancement by cathodic polarization at higher temperatures could be attributed to the reduced thermodynamic stability of the $AuPtO_x$ pre-formed in the aging process with increase of temperature. As a consequence, the activation energy of the electrochemical reduction of $AuPtO_x$ at the tpb (reaction 7) would be reduced. This and the general increase of reaction kinetics with temperature result in a quicker decomposition of $AuPtO_x$ by cathodic polarization ((Fig. 6b→c) at the highest temperature (700 °C) in the experiment. This enables a more effective and relatively thorough electrochemical reduction of $AuPtO_x$ at the tpb, which is in good agreement with the results reported in [72].

3.4. Study of cathodic polarization effects by CV and EIS measurements

Complementary CV and EIS measurements were conducted to prove these hypotheses. Fig. 8 shows the currents measured over the 1st, 3rd, 5th and 30th cyclic cathodic potential sweep on the APE at 700 °C under exposure to 5 vol.% O_2. The current is found to be slightly increased from the 1st to the 5th scan, while an extensively higher current is observed in the 30th scan. This is a clear indication that, the rate of the oxygen reduction reaction (ORR 3, Sec. 3.1) rises with the time of cathodic polarization on the APE (Fig. 6e). This rate is further enhanced by increasing the number of scans.

Moreover, Fig. 8 shows clearly that the hysteresis of these i-U envelope curves becomes considerably smaller when the number of cyclic potential sweeps increases. The larger hysteresis of the i-U envelope curves in the 1st, 3rd, and 5th scan indicates a relatively higher capacitive characteristic of the APE|YSZ interface. This is probably a consequence of the oxidation of the metallic parts of the tpb during the foregoing aging process (Fig. 6a→b). As already elucidated above (reaction 7), the cathodic polarization is postulated to facilitate the electrochemical reduction of those $AuPtO_x$ parts at the tpb (Fig. 6b→c). Correspondingly, this lowers the capacitive properties of the APE|YSZ interface, which is reflected by diminishing i-U hysteresis at simultaneously raised cathodic currents.

The EIS characteristics of the sensor (1#) were measured at the same intermediate states of the cathodic polarization treatments. Fig. 9 shows the EIS measurements of this aged sensor in synthetic air i) before the application of any polarization treatment, and ii) after cathodic polarization of the sensor at different temperatures between 600–700 °C at 5 vol.% O_2. After the 100 days sensor aging at 600 °C in ambient air but before any polarization treatment, the Nyquist plot is found to exhibit an incomplete quasi-semicircle in shape with the largest R_p in synthetic air at 600 °C compared with those measured after polarization under the
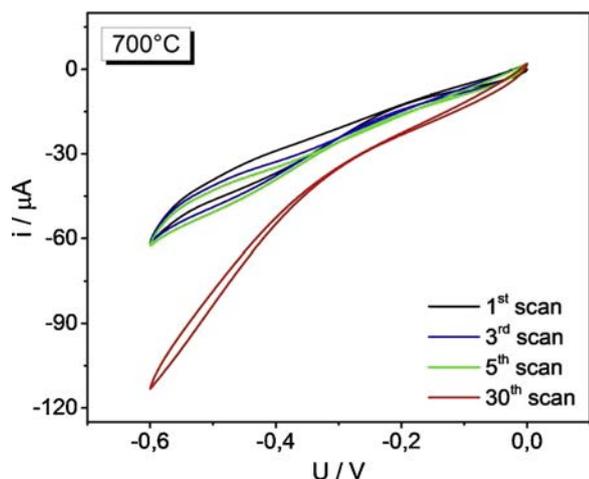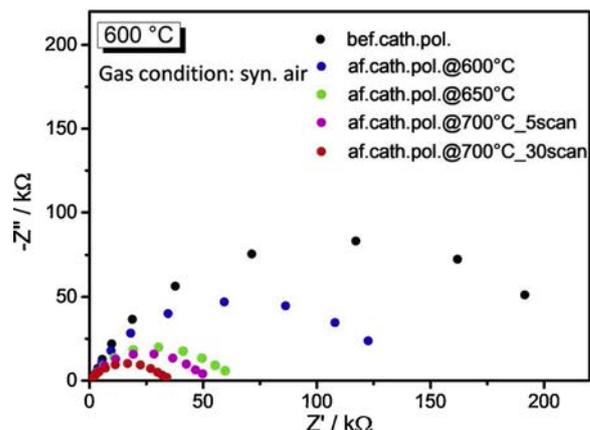
Fig. 9. EIS behaviors of the aged sensor1# at 600 °C in synthetic air before and after cathodic polarization treatments conducted at different temperatures.

same conditions.

By application of the cathodic polarization treatments at higher temperatures, and especially by increase of the number of scans at 700 °C, the Nyquist plots of the EIS characteristics tend more and more to show a shape of complete semicircle, and the corresponding R_p of those EIS semicircles become smaller and smaller. The opening at the incomplete semicircle is an indication of the phase shift between the AC-perturbance and the yielding AC-current across the tpb [74]. This phase shift is highly influenced by the capacitive behavior of the tpb at the APE. The change of the Nyquist plots in shape from incomplete to complete quasi-semicircle manifests that the APE|YSZ interface tends to be less capacitive after polarization. Another consequence of the cathodic polarization treatment is the enhancement of the oxygen reaction in thermodynamic equilibrium, which is indicated by the reduction of the R_p, i.e. the exchange current density for the oxygen reduction reaction gets increased. These experimental results again confirm that the improvement of the OCP response to CO (Fig. 7) is well correlated with the less capacitive but more conductive characteristics of the APE|YSZ interface.

The assumptions proposed in Fig. 6 are well supported by the changes observed in the CV (Fig. 8) and the EIS characteristics (Fig. 9) caused by polarization, and accordingly their correlation with the OCP response (Fig. 7). That is to say, the cathodic polarization facilitates the electrochemical reduction of the APE|YSZ interface (Fig. 6b→c). As already stated above, this leads to an increased concentration of the active electrochemical reaction sites at the tpb, and is correlated with a larger OCP response, namely, a stronger mixed-potential formation at the APE when exposed to CO/air mixtures. And, the regeneration effect of the cathodic polarization treatment on the APE by elevating the temperature is enhanced probably owing to the more distinct instability of the $AuPtO_x$ formed in the aging process at the tpb, and consequently the higher reaction kinetics of the corresponding electrochemical reduction process (reaction 7) at higher temperatures.

3.5. Influence of temperature treatment and oxygen concentration on response regeneration

As already shown in Fig. 7, the efficiency of the response recovery by cathodic polarization is highly affected by the sensor operation temperature, which is explained by the reduced thermodynamic stability of the $AuPtO_x$ formed in the aging process. It could be inferred that the regeneration of the sensing response might be (partly) realized by merely increasing the operation temperature. In order to better separate the roles of the operation temperature and the cathodic polarization treatment with respect to the efficiency of response regeneration, the response change of the sensor 1# after only the temperature treatment

Fig. 8. Cyclic voltammograms sampled in the 1st, 3rd, 5th and 30th scan in the cathodic polarization sequence of the aged APE (sensor 1#) at 700 °C under exposure to 5 vol.% O_2.

at 700 °C in synthetic air is compared with the change after the polarization treatment at 700 °C under exposure to 5 vol.% O_2 (Fig. 10). Moreover, the O_2 concentration in the gas atmosphere was also reported to take influence on the effect of electrode polarization [43,68]. This aspect was also studied in this work by investigation of the response regeneration effects on the sensor 2#, which was only polarized in synthetic air at the same temperature conditions (Sec. 2.3). The results are shown as relative sensitivities formulated as response change in percentage (Δresponse %) (Fig. 10) in accordance to Eq. (8)

$$\Delta response\ \% \quad \frac{\Delta\ U\ (measured)}{\Delta\ U\ (initial)} * 100\% \tag{8}$$

where ΔU is the sensing response to the CO/air mixture with 1000 ppm CO at 600 °C. After the aging process (Sec. 2.2), the ΔU of the sensor 1# was reduced to about 15 % of the value of the initial response. The degraded response could be elevated to approx. 32 % by raising the temperature of the sensor to 700 °C for 2 h in synthetic air. This is possibly attributed to the thermal decomposition of a part of $AuPtO_x$ formed at the tpb, which is assumed to block the mixed potential formation (Fig. 6 b&d).

A remarkable response recovery from 32 % to almost 100 % was observed within about twelve minutes of additional treatment of cathodic polarization at 5 vol.% O_2 at the same temperature (700 °C). These different efficiencies of regeneration indicate quite clearly, that the major driving force for the decomposition of the $AuPtO_x$ is the cathodic polarization at 700 °C, much more efficient than merely raising the temperature. In other words, only a small part of the $AuPtO_x$ at the tpb is thermally decomposed by simply heating up the sensor to 700 °C, but a quick and thorough decomposition is achieved when the oxide reduction process (reaction 7) in addition is electrochemically supported.

Furthermore, it was experimentally demonstrated that the effect of the cathodic polarization and the corresponding efficiency of the response regeneration are not dependent on the oxygen concentration of the gas atmosphere. The sensing response can be almost 100 % restored under the same polarization conditions, no matter whether the polarization is carried out in synthetic air (20.5 vol.% O_2) as shown for sensor 2# or at a reduced oxygen concentration (5 vol.% O_2) as revealed for sensor (1#) (Fig. 10). This aspect is of great importance because it opens possibilities of sensitivity regeneration during long term applications of this type of sensors.

4. Conclusions

The long term stability of a layered Au,Pt-YSZ mixed potential gas sensing electrode (APE) was studied by open circuit potentiometry (OCP), cyclic voltammetry (CV) and electrochemical impedance spectroscopy (EIS). The mixed potential response of such kind of electrode to CO was observed to be considerably reduced after an aging treatment of 100 days under ambient air conditions at 600 °C. This CO response degradation was found to be in good correlation with a clear loss of the electrode kinetics of oxygen involved reactions, as confirmed by EIS and CV measurements. Surprisingly, the degradation of mixed potential response and electrode kinetics is nearly fully regenerated after several cycles of cyclic cathodic polarization, but only at elevated operation temperatures (700 °C). This could be experimentally confirmed on several sensor elements of this type after different aging procedures. These experimental observations are explained by a theoretical model based on i) the oxidation of the electrode/electrolyte interface (triple phase boundary) due to aging processes and ii) the electrochemical reduction of those oxidized states by cathodic polarization, which is proposed for the first time in this paper. Due to the strong correlation of the mixed potential response to CO with the electrochemical impedance characteristic and the dynamic behavior (cathodic CV characteristic) in synthetic air, the combination of the EIS method with the cathodic
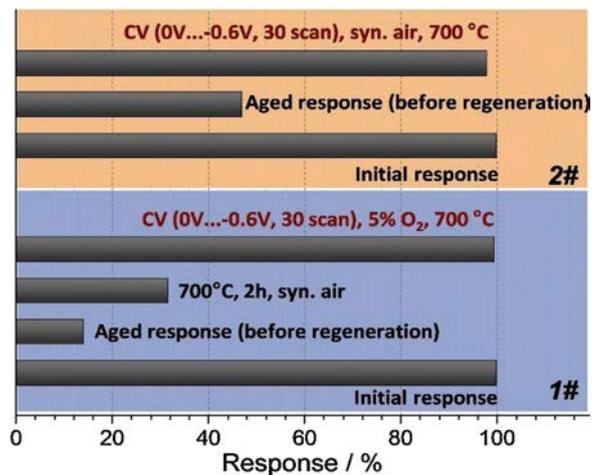
Fig. 10. Comparison of response regeneration of the two sensor individuals as a result of temperature treatment and cathodic polarization under different oxygen concentrations, separately.

polarization procedure is a very promising tool which enables sensitivity monitoring and, if necessary, sensor regeneration. The authors are optimistic that periodic application of this electrochemical procedure allows long-term in-situ high temperature applications of this kind of CO/HC-sensors, for instance in advanced wood-log combustion control systems to optimize the combustion process and lower the emission of un-combusted, mostly toxic gas components in flue gas. Experiments to prove this possibility have just been started.

CRediT authorship contribution statement

X. Zhang: Conceptualization, Methodology, Investigation, Validation, Formal analysis, Visualization, Writing - original draft. **H. Kohler:** Conceptualization, Methodology, Resources, Writing - review & editing, Supervision. **M. Schwotzer:** Investigation, Resources. **U. Guth:** Conceptualization, Writing - review & editing, Supervision.

Declaration of Competing Interest

The authors declare that they have no known competing financial interests or personal relationships that could have appeared to influence the work reported in this paper.

Acknowledgements

References

[1] P.K. Sekhar, E.L. Brosha, R. Mukundan, W. Li, M.A. Nelson, P. Palanisamy, F. H. Garzon, Application of commercial automotive sensor manufacturing methods for NOx/NH3 mixed potential sensors for on-board emissions control, Sens. Actuators B Chem. 144 (2010) 112–119, https://doi.org/10.1016/j. snb.2009.10.045.

[2] P. Butschbach, F. Hammer, H. Kohler, A. Potreck, T. Trautmann, Extensive reduction of toxic gas emissions of firewood-fueled low power fireplaces by improved in situ gas sensorics and catalytic treatment of exhaust gas, Sens. Actuators B Chem. 137 (2009) 32–41, https://doi.org/10.1016/j.snb.2008.12.007.

[3] E.L. Brosha, R. Mukundan, R. Lujan, F.H. Garzon, Mixed potential NOx sensors using thin film electrodes and electrolytes for stationary reciprocating engine type applications, Sens. Actuators B Chem. 119 (2006) 398–408, https://doi.org/ 10.1016/j.snb.2005.12.044.

[4] J. Riegel, H. Neumann, H.M. Wiedenmann, Exhaust gas sensors for automotive emission control, Solid State Ion. 152–153 (2002) 783–800, https://doi.org/ 10.1016/S0167-2738(02)00329-6.

[5] E.L. Brosha, R. Mukundan, D.R. Brown, F.H. Garzon, J.H. Visser, Development of ceramic mixed potential sensors for automotive applications, Solid State Ion. 148 (2002) 61–69, https://doi.org/10.1016/S0167-2738(02)00103-0.

[6] M. Fleischer, M. Lehmann, Solid State Gas Sensors-Industrial Application, Springer Science & Business Media, 2012.

[7] S. Zhuiykov, N. Miura, Development of zirconia-based potentiometric NOx sensors for automotive and energy industries in the early 21st century: what are the prospects for sensors? Sens. Actuators B Chem. 121 (2007) 639–651, https://doi.org/10.1016/j.snb.2006.03.044.

[8] N. Yamazoe, Toward innovations of gas sensor technology, Sens. Actuators B Chem. 108 (2005) 2–14, https://doi.org/10.1016/j.snb.2004.12.075.

[9] R. Moos, A brief overview on automotive exhaust gas sensors based on electroceramics, Int. J. Appl. Ceram. Technol. 2 (2005) 401–413.

[10] S. Capone, A. Forleo, L. Francioso, R. Rella, P. Siciliano, J. Spadavecchia, D. Presicce, A. Taurino, Solid state gas sensors: state of the art and future activities, J. Optoelectron. Adv. Mater. 5 (2003) 1335–1348.

[11] U. Guth, W. Vonau, J. Zosel, Recent developments in electrochemical sensor application and technology—a review, Meas. Sci. Technol. 20 (2009), 042002.

[12] C. Park, J. Fergus, N. Miura, J. Park, A. Choi, Solid-state electrochemical gas sensors, Ionics 15 (2009) 261–284.

[13] K. Rajeshwar, J.G. Ibanez, Environmental Electrochemistry: Fundamentals and Applications in Pollution Sensors and Abatement, Academic Press, 1997.

[14] E. Comini, G. Faglia, G. Sberveglieri, Solid State Gas Sensing, Springer Science & Business Media, 2008.

[15] M.J. Madou, S.R. Morrison, Chemical Sensing With Solid State Devices, Elsevier, 2012.

[16] B. Ojha, N. Illyaskutty, J. Knoblauch, M.R. Balachandran, H. Kohler, High-temperature CO/HC gas sensors to optimize firewood combustion in low-power fireplaces, J. Sens. Sens. Syst. 6 (2017) 237–246.

[17] H. Kohler, B. Ojha, N. Illyaskutty, I. Hartmann, C. Thiel, K. Eisinger, M. Dambacher, In situ high-temperature gas sensors: continuous monitoring of the combustion quality of different wood combustion systems and optimization of combustion process, J. Sens. Sens. Syst. 7 (2018) 161–167.

[18] H. Peters, H. Mobius, Elektrochemische Untersuchung der Gleichgewichte CO+ ½ O2⇌ CO2 und C+ CO2⇌ 2CO, Zeitschrift für Physikalische Chemie 209 (1958) 298–309.

[19] H. Peters, H. Mobius, Elektrochemische Untersuchung des Kohlensauredissoziations-gleichgewichtes und des Boudouard-Gleichgewichtes, Naturwissenschaften 45 (1958) 309–310.

[20] A.J. Bard, G. Inzelt, F. Scholz, Electrochemical Dictionary, Springer Science & Business Media, 2008.

[21] P.T. Moseley, Solid State Gas Sensors, Taylor & Francis, 1987.

[22] S. Zhuiykov, Electrochemistry of Zirconia Gas Sensors, CRC Press, 2007.

[23] R. Moos, K. Sahner, M. Fleischer, U. Guth, N. Barsan, U. Weimar, Solid state gas sensor research in Germany–a status report, Sensors 9 (2009) 4323–4365.

[24] U. Guth, P. Shuk, C. McGuire, Gas sensing technologies in combustion: a comprehensive review, J. Electrochem. Sci. Eng. 10 (2020) 103–110.

[25] I. Riess, Comparison Between Liquid State and Solid State Electrochemistry, Encyclopedia of Electrochemistry: Online, 2007.

[26] X. Zhang, H. Kohler, M. Schwotzer, Y.H. Wu, U. Guth, Mixed-potential gas sensor with layered Au,Pt-YSZ electrode: investigating the sensing mechanism with steady state and dynamic electrochemical methods, Sens. Actuators B Chem. 252 (2017) 554–560, https://doi.org/10.1016/j.snb.2017.05.168.

[27] T. Ueda, H. Abe, K. Kamada, S.R. Bishop, H.L. Tuller, T. Hyodo, Y. Shimizu, Enhanced sensing response of solid-electrolyte gas sensors to toluene: role of composite Au/metal oxide sensing electrode, Sens. Actuators B Chem. 252 (2017) 268–276, https://doi.org/10.1016/j.snb.2017.05.172.

[28] X. Zhang, H. Kohler, M. Schwotzer, U. Guth, Mixed-potential gas sensor with PtAu-8YSZ sensing electrode: electric potential difference measurements at isothermal and thermo-cyclic operation, Sens. Actuators B Chem. 217 (2015) 107–112, https://doi.org/10.1016/j.snb.2014.10.106.

[29] I. Romanytsia, J.-P. Viricelle, P. Vernoux, C. Pijolat, Application of advanced morphology Au–X (X ⯑ YSZ, ZrO2) composites as sensing electrode for solid state mixed-potential exhaust NOx sensor, Sens. Actuators B Chem. 207 (Part A) (2015) 391–397, https://doi.org/10.1016/j.snb.2014.10.017.

[30] M. Breedon, N. Miura, Augmenting H2 sensing performance of YSZ-based electrochemical gas sensors via the application of Au mesh and YSZ coating, Sens. Actuators B Chem. 182 (2013) 40–44, https://doi.org/10.1016/j.snb.2013.02.108.

[31] J. Zosel, M. Schelter, W. Oelßner, C. Vonau, U. Enseleit, U. Guth, M. Mertig, V. Voshook, D. Tuchtenhagen, K. Wienand, Recent developments in materials for potentiometric sensors, Proceedings IMCS 2012 (2012) 569–572.

[32] J. Zosel, G. Schiffel, F. Gerlach, K. Ahlborn, U. Sasum, V. Vashook, U. Guth, Electrode materials for potentiometric hydrogen sensors, Solid State Ion. 177 (2006) 2301–2304, https://doi.org/10.1016/j.ssi.2006.01.004.

[33] J. Zosel, R. Müller, V. Vashook, U. Guth, Response behavior of perovskites and Au/oxide composites as HC-electrodes in different combustibles, Solid State Ion. 175 (2004) 531–533, https://doi.org/10.1016/j.ssi.2004.01.074.

[34] J. Zosel, K. Ahlborn, R. Müller, D. Westphal, V. Vashook, U. Guth, Selectivity of HC-sensitive electrode materials for mixed potential gas sensors, Solid State Ion. 169 (2004) 115–119, https://doi.org/10.1016/S0167-2738(03)00082-1.

[35] J. Zosel, D. Westphal, S. Jakobs, R. Müller, U. Guth, Au–oxide composites as HC-sensitive electrode material for mixed potential gas sensors, Solid State Ion. 152–153 (2002) 525–529, https://doi.org/10.1016/S0167-2738(02)00355-7.

[36] T. Striker, V. Ramaswamy, E.N. Armstrong, P.D. Willson, E.D. Wachsman, J. A. Ruud, Effect of nanocomposite Au–YSZ electrodes on potentiometric sensor response to NO x and CO, Sens. Actuators B Chem. 181 (2013) 312–318.

[37] S.A. Anggraini, V.V. Plashnitsa, P. Elumalai, M. Breedon, N. Miura, Stabilized zirconia-based planar sensor using coupled oxide (+ Au) electrodes for highly selective CO detection, Sens. Actuators B Chem. 160 (2011) 1273–1281.

[38] R.-J. Wu, C.-H. Hu, C.-T. Yeh, P.-G. Su, Nanogold on powdered cobalt oxide for carbon monoxide sensor, Sens. Actuators B Chem. 96 (2003) 596–601.

[39] X. Zhang, H. Kohler, M. Schwotzer, Y. Wu, U. Guth, Study of a Layered Au, Pt-YSZ Mixed-potential Sensing Electrode by ESEM, XRD and GD-OES With Relation to Its Electrochemical Behaviour, Multidisciplinary Digital Publishing Institute Proceedings, 2017, p. 465.

[40] X. Zhang, H. Kohler, M. Schwotzer, Y. Wu, U. Guth, Layered Au, Pt-YSZ mixed potential gas sensing electrode: Correlation among sensing response, dynamic electrochemical behavior and structural properties, Sens. Actuators B Chem. 278 (2019) 117–125.

[41] X. Zhang, Electrochemical and Structural Investigations of a Layered AU,PT-YSZ Mixed Potential Gas Sensing Electrode [Doctoral dissertation], Technische Universitat Dresden, 2019.

[42] F.H. Garzon, R. Mukundan, E.L. Brosha, Solid-state mixed potential gas sensors: theory, experiments and challenges, Solid State Ion. 136–137 (2000) 633–638, https://doi.org/10.1016/S0167-2738(00)00348-9.

[43] H. Popke, E. Mutoro, B. Luerssen, J. Janek, Oxidation of platinum in the epitaxial model system Pt (111)/YSZ (111): quantitative analysis of an electrochemically driven PtO x formation, J. Phys. Chem. C 116 (2012) 1912–1920.

[44] A.K. Opitz, M.P. Horlein, T. Huber, J. Fleig, Current-voltage characteristics of platinum model electrodes on yttria-stabilized zirconia, J. Electrochem. Soc. 159 (2012) B502–B513.

[45] T. Ryll, H. Galinski, L. Schlagenhauf, P. Elser, J.L. Rupp, A. Bieberle-Hutter, L. J. Gauckler, Microscopic and nanoscopic three-phase-boundaries of platinum thin-film electrodes on YSZ electrolyte, Adv. Funct. Mater. 21 (2011) 565–572.

[46] H. Popke, E. Mutoro, C. Raiß, B. Luerßen, M. Amati, M.K. Abyaneh, L. Gregoratti, J. Janek, The role of platinum oxide in the electrode system Pt(O2)/yttria-stabilized zirconia, Electrochim. Acta 56 (2011) 10668–10675, https://doi.org/10.1016/j.electacta.2011.04.057.

[47] H. Popke, E. Mutoro, B. Luerßen, J. Janek, The potential of in situ-scanning electron microscopy — morphology changes of electrically polarized thin film Pt (O2)/YSZ model electrodes, Solid State Ion. 189 (2011) 56–62, https://doi.org/10.1016/j.ssi.2011.02.021.

[48] A.K. Opitz, A. Lutz, M. Kubicek, F. Kubel, H. Hutter, J. Fleig, Investigation of the oxygen exchange mechanism on Pt|yttria stabilized zirconia at intermediate temperatures: surface path versus bulk path, Electrochim. Acta 56 (2011) 9727–9740, https://doi.org/10.1016/j.electacta.2011.07.112.

[49] A. Kumar, F. Ciucci, A.N. Morozovska, S.V. Kalinin, S. Jesse, Measuring oxygen reduction/evolution reactions on the nanoscale, Nat. Chem. 3 (2011) 707.

[50] G. Beck, H. Popke, B. Luerßen, J. Janek, Microstructure of platinum films on YSZ prepared by pulsed laser deposition, J. Cryst. Growth 322 (2011) 95–102, https://doi.org/10.1016/j.jcrysgro.2011.02.046.

[51] A.K. Opitz, A. Schintlmeister, H. Hutter, J. Fleig, Visualization of oxygen reduction sites at Pt electrodes on YSZ by means of 18O tracer incorporation: the width of the electrochemically active zone, J. Chem. Soc. Faraday Trans. 12 (2010) 12734–12745.

[52] A.K. Opitz, J. Fleig, Investigation of O2 reduction on Pt/YSZ by means of thin film microelectrodes: the geometry dependence of the electrode impedance, Solid State Ion. 181 (2010) 684–693, https://doi.org/10.1016/j.ssi.2010.03.017.

[53] E. Mutoro, N. Baumann, J.r. Janek, Janus-faced SiO2: activation and passivation in the electrode system platinum/yttria-stabilized zirconia, J. Phys. Chem. Lett. 1 (2010) 2322–2326.

[54] N. Baumann, E. Mutoro, J. Janek, Porous model type electrodes by induced dewetting of thin Pt films on YSZ substrates, Solid State Ion. 181 (2010) 7–15, https://doi.org/10.1016/j.ssi.2009.11.019.

[55] E. Mutoro, B. Luerßen, S. Günther, J. Janek, The electrode model system Pt(O2)| YSZ: influence of impurities and electrode morphology on cyclic voltammograms, Solid State Ion. 180 (2009) 1019–1033, https://doi.org/10.1016/j.ssi.2009.04.012.

[56] J.L. Hertz, A. Rothschild, H.L. Tuller, Highly enhanced electrochemical performance of silicon-free platinum–yttria stabilized zirconia interfaces, J. Electroceram. 22 (2009) 428–435.

[57] G. Fóti, A. Jaccoud, C. Falgairette, C. Comninellis, Charge storage at the Pt/YSZ interface, J. Electroceram. 23 (2009) 175.

[58] C. Falgairette, G. Fóti, Oxygen storage in O2/Pt/YSZ cell, Catal. Today 146 (2009) 274–278, https://doi.org/10.1016/j.cattod.2009.05.004.

[59] E. Mutoro, S. Günther, B. Luerßen, I. Valov, J. Janek, Electrode activation and degradation: morphology changes of platinum electrodes on YSZ during electrochemical polarisation, Solid State Ion. 179 (2008) 1835–1848, https://doi.org/10.1016/j.ssi.2008.05.007.

[60] S. Koc, G.J. La O, T. Golfinopoulos, Y. Shao-Horn, Impedance spectroscopy studies of oxygen reduction reaction on thin film platinum microelectrodes supported on YSZ, ECS Trans. 7 (2007) 1271–1277.

[61] E. Flegel, Charakterisierungsmethoden für das Alterungsverhalten von O2,Pt|YSZ-Elektroden für Gassensoren [Doctoral dissertation], Technische Universitat Dresden, 2019.

[62] J. Janek, B. Luerßen, E. Mutoro, H. Fischer, S. Günther, In situ imaging of electrode processes on solid electrolytes by photoelectron microscopy and microspectroscopy–the role of the three-phase boundary, Top. Catal. 44 (2007) 399–407.

[63] R. Radhakrishnan, A.V. Virkar, S.C. Singhal, Estimation of charge-transfer resistivity of Pt cathode on YSZ electrolyte using patterned electrodes, J. Electrochem. Soc. 152 (2005) A927–A936.

[64] N. Kotsionopoulos, S. Bebelis, Electrochemical promotion of the oxidation of propane on Pt/YSZ and Rh/YSZ catalyst-electrodes, J. Appl. Electrochem. 35 (2005) 1253–1264.

[65] S.B. Adler, Factors governing oxygen reduction in solid oxide fuel cell cathodes, Chem. Rev. 104 (2004) 4791–4844.

[66] N.Q. Minh, Ceramic fuel cells, J. Am. Ceram. Soc. 76 (1993) 563–588.

[67] C. Vayenas, S. Bebelis, I. Yentekakis, P. Tsiakaras, H. Karasali, Non-faradaic electrochemical modification of catalytic activity, Platin. Met. Rev. 34 (1990) 122–130.

[68] C. Vayenas, S. Bebelis, S. Ladas, Dependence of catalytic rates on catalyst work function, Nature 343 (1990) 625–627.

[69] A. Mitterdorfer, L. Gauckler, Identification of the reaction mechanism of the Pt, O2 (g)| yttria-stabilized zirconia system: part II: model implementation, parameter estimation, and validation, Solid State Ion. 117 (1999) 203–217.

[70] A. Mitterdorfer, L. Gauckler, Identification of the reaction mechanism of the Pt, O2 (g)| yttria-stabilized zirconia system: part I: general framework, modelling, and structural investigation, Solid State Ion. 117 (1999) 187–202.

[71] H. Popke, E. Mutoro, B. Luerßen, J. Janek, Oxygen reduction and oxidation at epitaxial model-type Pt(O2)/YSZ electrodes – on the role of PtOx formation on activation, passivation, and charge transfer, Catal. Today 202 (2013) 12–19, https://doi.org/10.1016/j.cattod.2012.02.058.

[72] M.P. Horlein, A.K. Opitz, J. Fleig, On the variability of oxygen exchange kinetics of platinum model electrodes on yttria stabilized zirconia, Solid State Ion. 247 (2013) 56–65.

[73] S. Sridhar, V. Stancovski, U.B. Pal, Effect of oxygen-containing species on the impedance of the Pt/YSZ interface, Solid State Ion. 100 (1997) 17–22.

[74] J.R. Macdonald, W.R. Kenan, Impedance Spectroscopy: Emphasizing Solid Materials and Systems, Wiley, 1987.

[75] N. Miura, T. Sato, S. Anggraini, H. Ikeda, S. Zhuiykov, A review of mixed-potential type zirconia-based gas sensors, Ionics 20 (2014) 901–925, https://doi.org/10.1007/s11581-014-1140-1.

[76] G. Lu, N. Miura, N. Yamazoe, High-temperature hydrogen sensor based on stabilized zirconia and a metal oxide electrode, Sens. Actuators B Chem. 35 (1996) 130–135, https://doi.org/10.1016/S0925-4005(97)80042-1.

[77] N. Miura, T. Raisen, G. Lu, N. Yamazoe, Highly selective CO sensor using stabilized zirconia and a couple of oxide electrodes, Sens. Actuators B Chem. 47 (1998) 84–91.

[78] L.Y. Woo, L.P. Martin, R.S. Glass, R.J. Gorte, Impedance characterization of a model Au∕ yttria-stabilized zirconia∕ Au electrochemical cell in varying oxygen and NO x concentrations, J. Electrochem. Soc. 154 (2007) J129–J135.

Xin Zhang was graduated in sensor system technology from Karlsruhe University of Applied Sciences, and afterwards received his Ph.D from Dresden University of Technology. He is working now as a research scientist in LAMTEC Meß- und Regeltechnik für Feuerungen GmbH & Co KG. His current research interests include chemical sensors, sensor technology and intelligent gas sensor systems.

Heinz Kohler graduated in physics (1975–1981) at Karlsruhe Technical University, Germany. Afterwards he had a doctoral fellowship at the Max-Planck Institute of Solid State Research, Stuttgart (1981–1984) and received his doctoral degree from Karlsruhe Technical University in 1984. From 1984–1992 he had a position at Endress+Hauser Conducta GmbH as the head of a chemical sensor research group with main activities in sensors for field chemical analysis of liquids. Since 1992, he is working as Professor of Physics and Chemical Sensors at Karlsruhe University of Applied Sciences, Germany. His research interests include chemical sensor concepts and materials, sensor technology and intelligent gas sensor systems.

Matthias Schwotzer is graduated in mineralogy and received his Ph.D. in 2008 from Karlsruhe Institute of Technology (KIT), Germany for his research on the mechanisms of deterioration reactions of cement based materials exposed to various aqueous environments. Currently, he is the team leader of the research group "reactive transport processes" at the Institute of Functional Interfaces at KIT. His research interests are durability and functionalization of porous mineral materials, with focus on the chemical stability in aggressive aqueous environments. He is a co-founder of the spin of company IONYS AG – chemistry in engineering for durable constructions.

Ulrich Guth received his PhD from the University of Greifswald in 1975. In 1993 he became a professor for solid state chemistry at the University of Greifswald. From 1999–2010 he had been working as the director of the Meinsberg Kurt-Schwabe Research Institute and as a professor for physical chemistry especially sensor and measuring technology at the Dresden University of Technology. His principal research interests are directed towards solid electrolyte sensors and new materials for these high temperature sensors.